arXiv:0811.0088v3 [hep-ex] 9 Feb 2009

BELLE Preprint 2008-28
KEK Preprint 2008-38
NTLP 2008-03
arXiv:0811.0088 [hep-ex]

Precise measurement of hadronic τ-decays with an η meson

Belle Collaboration

K. Inami [s], T. Ohshima [s], H. Kaji [s], I. Adachi [f], H. Aihara [ak],
K. Arinstein [a], V. Aulchenko [a], T. Aushev [o,j], I. Bedny [a],
V. Bhardwaj [ac], A. Bondar [a], M. Bračko [q,k], T. E. Browder [e],
M.-C. Chang [b], Y. Chao [w], R. Chistov [j], I.-S. Cho [ao], Y. Choi [ag],
J. Dalseno [f], M. Dash [an], S. Eidelman [a], D. Epifanov [a],
N. Gabyshev [a], B. Golob [p,k], J. Haba [f], K. Hara [s], K. Hayasaka [s],
H. Hayashii [t], D. Heffernan [ab], Y. Hoshi [aj], W.-S. Hou [w],
H. J. Hyun [n], T. Iijima [s], A. Ishikawa [ad], Y. Iwasaki [f],
D. H. Kah [n], J. H. Kang [ao], T. Kawasaki [y], H. Kichimi [f],
H. O. Kim [n], S. K. Kim [af], Y. I. Kim [n], Y. J. Kim [d],
P. Krokovny [f], R. Kumar [ac], A. Kuzmin [a], Y.-J. Kwon [ao],
S.-H. Kyeong [ao], J. S. Lange [c], J. S. Lee [ag], M. J. Lee [af],
S. E. Lee [af], A. Limosani [r], S.-W. Lin [w], R. Louvot [o], F. Mandl [i],
S. McOnie [ah], T. Medvedeva [j], K. Miyabayashi [t], H. Miyata [y],
Y. Miyazaki [s], R. Mizuk [j], E. Nakano [aa], M. Nakao [f],
H. Nakazawa [u], O. Nitoh [am], S. Noguchi [t], S. Ogawa [ai],
S. Okuno [ℓ], H. Ozaki [f], P. Pakhlov [j], G. Pakhlova [j],
C. W. Park [ag], H. Park [n], H. K. Park [n], K. S. Park [ag],
L. S. Peak [ah], L. E. Piilonen [an], A. Poluektov [a], Y. Sakai [f],
O. Schneider [o], M. Shapkin [h], V. Shebalin [a], J.-G. Shiu [w],
B. Shwartz [a], J. B. Singh [ac], S. Stanič [z], M. Starič [k],
T. Sumiyoshi [aℓ], M. Tanaka [f], G. N. Taylor [r], Y. Teramoto [aa],
S. Uehara [f], T. Uglov [j], S. Uno [f], Y. Usov [a], Y. Usuki [s],
G. Varner [e], A. Vinokurova [a], C. H. Wang [v], P. Wang [g],
X. L. Wang [g], Y. Watanabe [ℓ], R. Wedd [r], E. Won [m],

Y. Yamashita [x], Z. P. Zhang [ae], V. Zhilich [a], V. Zhulanov [a], T. Zivko [k], A. Zupanc [k], and O. Zyukova [a],

[a] *Budker Institute of Nuclear Physics, Novosibirsk, Russia*
[b] *Department of Physics, Fu Jen Catholic University, Taipei, Taiwan*
[c] *Justus-Liebig-Universität Gießen, Gießen, Germany*
[d] *The Graduate University for Advanced Studies, Hayama, Japan*
[e] *University of Hawaii, Honolulu, HI, USA*
[f] *High Energy Accelerator Research Organization (KEK), Tsukuba, Japan*
[g] *Institute of High Energy Physics, Chinese Academy of Sciences, Beijing, PR China*
[h] *Institute for High Energy Physics, Protvino, Russia*
[i] *Institute of High Energy Physics, Vienna, Austria*
[j] *Institute for Theoretical and Experimental Physics, Moscow, Russia*
[k] *J. Stefan Institute, Ljubljana, Slovenia*
[ℓ] *Kanagawa University, Yokohama, Japan*
[m] *Korea University, Seoul, South Korea*
[n] *Kyungpook National University, Taegu, South Korea*
[o] *École Polytechnique Fédérale de Lausanne, EPFL, Lausanne, Switzerland*
[p] *Faculty of Mathematics and Physics, University of Ljubljana, Ljubljana, Slovenia*
[q] *University of Maribor, Maribor, Slovenia*
[r] *University of Melbourne, Victoria, Australia*
[s] *Nagoya University, Nagoya, Japan*
[t] *Nara Women's University, Nara, Japan*
[u] *National Central University, Chung-li, Taiwan*
[v] *National United University, Miao Li, Taiwan*
[w] *Department of Physics, National Taiwan University, Taipei, Taiwan*
[x] *Nippon Dental University, Niigata, Japan*
[y] *Niigata University, Niigata, Japan*
[z] *University of Nova Gorica, Nova Gorica, Slovenia*
[aa] *Osaka City University, Osaka, Japan*
[ab] *Osaka University, Osaka, Japan*
[ac] *Panjab University, Chandigarh, India*
[ad] *Saga University, Saga, Japan*
[ae] *University of Science and Technology of China, Hefei, PR China*
[af] *Seoul National University, Seoul, South Korea*
[ag] *Sungkyunkwan University, Suwon, South Korea*

[ah] *University of Sydney, Sydney, NSW, Australia*
[ai] *Toho University, Funabashi, Japan*
[aj] *Tohoku Gakuin University, Tagajo, Japan*
[ak] *Department of Physics, University of Tokyo, Tokyo, Japan*
[aℓ] *Tokyo Metropolitan University, Tokyo, Japan*
[am] *Tokyo University of Agriculture and Technology, Tokyo, Japan*
[an] *IPNAS, Virginia Polytechnic Institute and State University, Blacksburg, VA, USA*
[ao] *Yonsei University, Seoul, South Korea*

Abstract

We have studied hadronic τ decay modes involving an η meson using 490 fb^{-1} of data collected with the Belle detector at the KEKB asymmetric-energy e^+e^- collider. The following branching fractions have been measured: $\mathcal{B}(\tau^- \to K^-\eta\nu_\tau) = (1.58 \pm 0.05 \pm 0.09) \times 10^{-4}$, $\mathcal{B}(\tau^- \to K^-\pi^0\eta\nu_\tau) = (4.6 \pm 1.1 \pm 0.4) \times 10^{-5}$, $\mathcal{B}(\tau^- \to \pi^-\pi^0\eta\nu_\tau) = (1.35 \pm 0.03 \pm 0.07) \times 10^{-3}$, $\mathcal{B}(\tau^- \to \pi^-K^0_S\eta\nu_\tau) = (4.4 \pm 0.7 \pm 0.2) \times 10^{-5}$, and $\mathcal{B}(\tau^- \to K^{*-}\eta\nu_\tau) = (1.34 \pm 0.12 \pm 0.09) \times 10^{-4}$. These results are substantially more precise than previous measurements. The new measurements are compared with theoretical calculations based on the CVC hypothesis or the chiral perturbation theory. We also set upper limits on branching fractions for τ decays into $K^-K^0_S\eta\nu_\tau$, $\pi^-K^0_S\pi^0\eta\nu_\tau$, $K^-\eta\eta\nu_\tau$, $\pi^-\eta\eta\nu_\tau$ and non-resonant $K^-\pi^0\eta\nu_\tau$ final states.

1 Introduction

Hadronic decays of the τ lepton are very important for studying QCD phenomena at a low-energy scale. Various decay modes including an η-meson represent a wide class of such decays, which are still poorly studied. One of the important tasks in this field is to test effective chiral theories [1,2,3,4]. The τ decay amplitudes in these theories are based on an effective Lagrangian of pseudoscalar, vector and axial-vector mesons with $U(3)_L \times U(3)_R$ symmetry. On the other hand, for some decays the branching fractions as well as spectral functions of the final states can be predicted using the vector dominance model (VDM). Another important issue is testing the relations between the cross section of $e^+e^- \to \pi^+\pi^-\eta$ and the spectral function in $\tau^- \to \pi^-\pi^0\eta\nu_\tau$ decay predicted by conservation of vector current (CVC) and isospin symmetry [5]. For all of the above tasks, precise measurements of the branching fractions as well as detailed studies of the final-state invariant mass distributions are highly desirable.

Three τ-decay modes involving η mesons, $\tau^- \to K^-\eta\nu_\tau$ [1], $\tau^- \to K^*(892)^-\eta\nu_\tau$, and $\tau^- \to \pi^-\pi^0\eta\nu_\tau$, have been studied by CLEO [6,7,8] and ALEPH [9]. However, the experimental statistics were very limited. For example, CLEO has the most precise measurements with 85 events in the $\tau^- \to K^-\eta\nu_\tau$ mode, 125 events in the $\tau^- \to \pi^-\pi^0\eta\nu_\tau$ mode and 25 in the $\tau^- \to K^{*-}\eta\nu_\tau$ mode. The limited statistics of these measurements result in large uncertainties for the branching fractions and do not allow study of the hadronic mass spectra.

We report a detailed study of the branching fractions for $\tau^- \to K^-\eta\nu_\tau$, $K^-\pi^0\eta\nu_\tau$, $\pi^-\pi^0\eta\nu_\tau$, as well as $\pi^-K_S^0\eta\nu_\tau$ decays. The $K^-\pi^0$ invariant mass in the $K^-\pi^0\eta\nu_\tau$ decay and the $\pi^-K_S^0$ invariant mass in the $\pi^-K_S^0\eta\nu_\tau$ decay are studied to evaluate the branching fraction of the $\tau^- \to K^*(892)^-\eta\nu_\tau$ decay. In addition, some other final-state invariant mass distributions are presented and discussed.

This study was performed at the KEKB asymmetric-energy e^+e^- collider [10] with the Belle detector. The results are based on a 490 fb^{-1} data sample that contains about 450 million τ-pairs, which is almost 100 times larger than in any of the previous measurements.

The structure of this paper is as follows. Section 2 describes the Belle detector. Event selection is explained in Section 3. The branching fractions are determined in Section 4, where that of $\tau^- \to K^*(892)^-\eta\nu_\tau$ is evaluated from analysis of the $\tau^- \to K^-\pi^0\eta\nu_\tau$ and $\pi^-K_S^0\eta\nu_\tau$ samples in Section 4.3. Finally, some concluding remarks are given in Section 5.

2 Experimental apparatus and Monte-Carlo simulation

The Belle detector is a large-solid-angle magnetic spectrometer that consists of a silicon vertex detector (SVD), a 50-layer central drift chamber (CDC), an array of aerogel threshold Cherenkov counters (ACC), a barrel-like arrangement of time-of-flight scintillation counters (TOF), and an electromagnetic calorimeter (ECL) comprised of CsI(Tl) crystals located inside a superconducting solenoid coil that provides a 1.5 T magnetic field. An iron flux-return located outside the coil is instrumented to detect K_L^0 mesons and to identify muons (KLM). The detector is described in detail elsewhere [11]. Two inner detector configurations were used. A 2.0 cm radius beam pipe and a 3-layer silicon vertex detector were used for the first sample of 140 fb^{-1}, while a 1.5 cm radius beam pipe, a 4-layer silicon detector and a small-cell inner drift chamber were used to record the remaining 350 fb^{-1} [12].

---

[1] Unless specified otherwise, charge-conjugate decays are implied throughout the paper.

Particle identification (PID) of the charged tracks uses likelihood ratios, $\mathcal{P}_x$, for a charged particle of species x ($x = \mu,\ e,\ K,\ \pi$ or p). $\mathcal{P}_x$ is defined as $\mathcal{P}_x = L_x/\Sigma_y L_y$ (the sum runs over the relevant particle species), where L_x is a likelihood based on the energy deposit and shower shape in the ECL, the momentum and dE/dX measured in the CDC, the particle range in the KLM, the light yield in the ACC, and the particle's time-of-flight from the TOF counter [13]. The efficiencies for kaon, muon and electron identification are 77% for momenta of $p > 0.3$ GeV/c, 92% for $p > 1.0$ GeV/c and 94% for $p > 0.5$ GeV/c, respectively.

The detection efficiency for each signal mode and the level of background (BG) contribution are estimated from Monte Carlo (MC) simulations. To generate signal events as well as τ-decay backgrounds, the KKMC program [14] is used. For the decay modes not covered by KKMC, like $\tau^- \to K^-\eta\nu_\tau$, $K^*(892)^-\eta\nu_\tau$, ..., the signal MC is produced assuming a pure phase-space distribution of the hadronic system with a $V-A$ weak interaction. The background from $e^+e^- \to q\bar{q}$ ($q\bar{q}$ continuum) is simulated using the EvtGen procedure [15]. The detector response is simulated by a GEANT3 [16] based program. Throughout the paper the efficiencies quoted include the branching ratios of the corresponding η decays.

3 Event Selections

The signal events should have the following common features in the $e^+e^- \to \tau^-_{\rm signal}\tau^+_{\rm tag}$ reaction:

$$\begin{aligned} \tau^-_{\rm signal} &\to X^- + \eta + n(\leq 1)\gamma + ({\rm missing}), \\ \tau^+_{\rm tag} &\to (\mu/e)^+ + n(\leq 1)\gamma + ({\rm missing}), \end{aligned}$$

where X^- denotes K^-, $K^-\pi^0$, $\pi^-\pi^0$, $\pi^-K^0_S$ or $K^*(892)^-$ systems. The π^0, K^0_S and $K^*(892)^-$ are reconstructed through $\pi^0 \to \gamma\gamma$, $K^0_S \to \pi^+\pi^-$, and $K^*(892)^- \to K^0_S\pi^-, K^-\pi^0$ decays, respectively. The η meson is identified through the $\eta \to \gamma\gamma$ decay mode for all τ channels while the $\eta \to \pi^+\pi^-\pi^0$ mode is added for the $\tau^- \to K^-\eta\nu$ decay mode.

The signal events, therefore, comprise either two or four charged tracks with zero net charge and two or four γ's. In order to take into account initial-state radiation, we allow at most one extra γ on both the signal and tag sides. Each charged track is required to have a transverse momentum $p_t > 0.1$ GeV/c, and a polar angle of $-0.866 < \cos\theta < 0.956$, where p_t and θ are measured relative to the direction opposite to that of the incident e^+ beam in the laboratory frame. Each photon candidate should have an energy $E_\gamma > 0.05$ GeV within the same polar angle region as for the charged particles.

The tag-side τ_{tag} is required to decay into leptons, i.e. $\tau^+ \to \ell^+\nu_\ell\bar{\nu}_\tau$ ($\ell = e/\mu$), which corresponds to a branching fraction of 35.2% [17]. The lepton candidates are required to be well identified by requirements on the $\mathcal{P}_e$ or $\mathcal{P}_\mu$ PID parameters with $p > 0.7$ GeV/c.

The thrust axis ($\mathbf{n}_{\text{thrust}}$) is defined to maximize $V_{\text{thrust}} = \Sigma_i|\mathbf{p}_i^{\text{CM}}\cdot\mathbf{n}_{\text{thrust}}|/\Sigma_i|\mathbf{p}_i^{\text{CM}}|$, where $\mathbf{p}_i^{\text{CM}}$ denotes the momentum of each particle in the center-of-mass system (CM), and the sum runs over all detected particles in an event. The requirement $V_{\text{thrust}} > 0.8$ is applied to remove $q\bar{q}$ events. An event is divided into two hemispheres by the plane perpendicular to $\mathbf{n}_{\text{thrust}}$. The hemisphere that includes τ_{signal} with an η is referred to as the signal side, while the opposite hemisphere, which includes τ_{tag}, is defined as the tag side.

In order to remove non-τ pair backgrounds, such as the $q\bar{q}$ continuum, the total energy in CM is required to be in the range 3.0 GeV $< E_{\text{total}}^{\text{CM}} <$ 10.0 GeV. In addition, the invariant masses of both the signal and the tag sides are required to be smaller than the τ-mass: $M_{\text{sig}},\ M_{\text{tag}} < m_\tau$ (1.78 GeV/c^2). To remove two-photon backgrounds, the missing momentum should correspond to a particle crossing the fiducial region; we require that the missing momentum satisfy $-0.866 < \cos\theta(p_{\text{miss}}) < 0.956$. After applying these requirements, the $q\bar{q}$ background level is 3% of the signal yield. Background from two-photon reactions is negligible.

To reconstruct an η, two γ's with $E_\gamma > 0.2$ GeV are required in the barrel region ($-0.624 < \cos\theta < 0.833$). In addition, we allow combinations with at most one extra γ with $0.05 < E_\gamma < 0.2$ GeV in the endcap region on the signal side to take into account initial-state radiation as well as beam-induced BG clusters in the calorimeter. In order to reduce the number of incorrect combinations with a γ from π^0 decay (denoted hereafter as γ_{π^0}), the η-candidate γ (γ_η) should not form a π^0 mass with any other γ, i.e., a π^0-veto is applied. The π^0 mass window is defined in this paper as 0.105 GeV/c^2 $< M_{\gamma\gamma} <$ 0.165 GeV/c^2, which is a $\pm3\sigma$ range of the detector resolution.

3.1 $\tau^- \to K^-\eta\nu_\tau$ decay

Candidate events for this decay mode must contain one charged track and at least two γ's in the $\eta \to \gamma\gamma$ case, or three charged tracks and two γ's in the $\eta \to \pi^+\pi^-\pi^0$ ($\pi^0 \to \gamma\gamma$) case.

A kaon is identified by the $\mathcal{P}_K$ parameter with $p > 0.3$ GeV/c. In addition, a low $\mathcal{P}_e$ value is required to remove beam electrons from two-photon processes; this requirement reduces two-photon BG to a negligible level. The opening angle between the K^- and η is required to satisfy the condition $\cos\theta(P_K^{\text{CM}}; P_\eta^{\text{CM}}) > 0.8$, to reduce the combinatorial BG. In addition, the

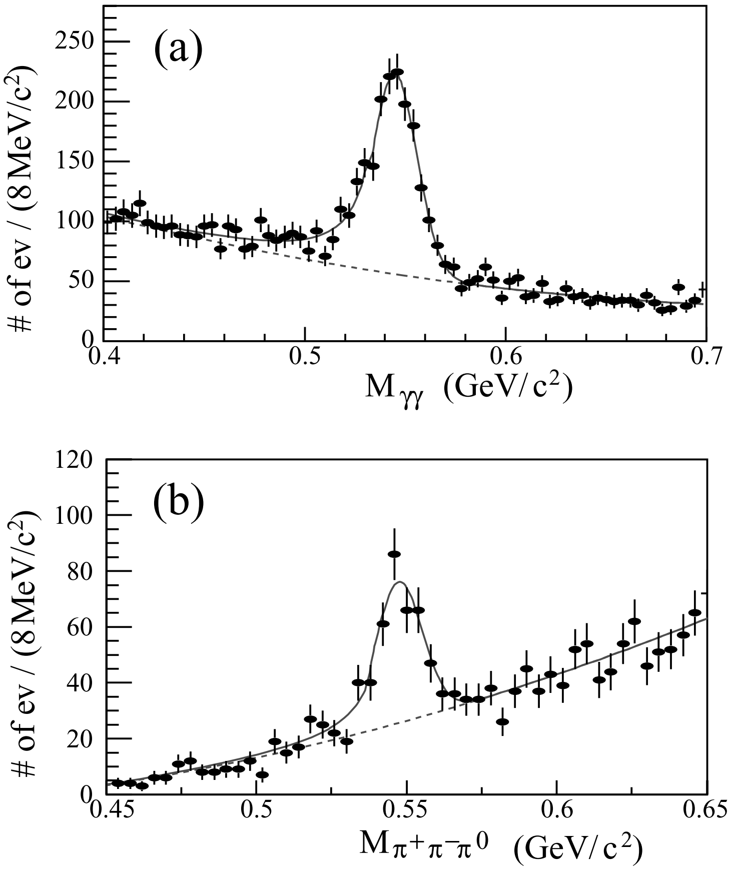

Fig. 1. (a) $M_{\gamma\gamma}$ and (b) $M_{\pi^+\pi^-\pi^0}$ distributions for $K^-\eta\nu_\tau$ selection in $\eta \to \gamma\gamma$ and $\eta \to \pi^-\pi^+\pi^0$ decays, respectively. Data are fit with a Crystal Ball function plus a second-order polynomial for the BG. The best-fit result is indicated by the solid curve with the BG shown by the dashed curve.

opening angle and energy of the two γ_η's should fulfill the following conditions: $0.5 < \cos\theta(P^{\rm CM}_{\gamma 1}; P^{\rm CM}_{\gamma 2}) < 0.96$ and $|E^{\rm CM}_{\gamma 1} - E^{\rm CM}_{\gamma 2}|/|E^{\rm CM}_{\gamma 1} + E^{\rm CM}_{\gamma 2}| < 0.8$, respectively.

For $\eta \to \pi^+\pi^-\pi^0$ reconstruction, the selection criteria are basically the same as in the $\eta \to \gamma\gamma$ case. Here η candidates should have two additional charged tracks, and two of the γ's must form a π^0 instead of an η.

The $\gamma\gamma$ and $\pi^+\pi^-\pi^0$ invariant mass distributions around η mass are shown in Figs.1 (a) and (b), respectively. The η peak is clearly seen in both cases. The selection efficiencies (including the intermediate branching fractions of $\mathcal{B}(\eta \to \gamma\gamma)$, $\mathcal{B}(\eta \to \pi^+\pi^-\pi^0)$, and $\mathcal{B}(\tau^- \to \ell^-\nu_\tau\bar{\nu}_\ell)$) are $\epsilon = 0.94\%$ in the $\eta \to \gamma\gamma$ and $\epsilon = 0.16\%$ in the $\eta \to \pi^+\pi^-\pi^0$ case.

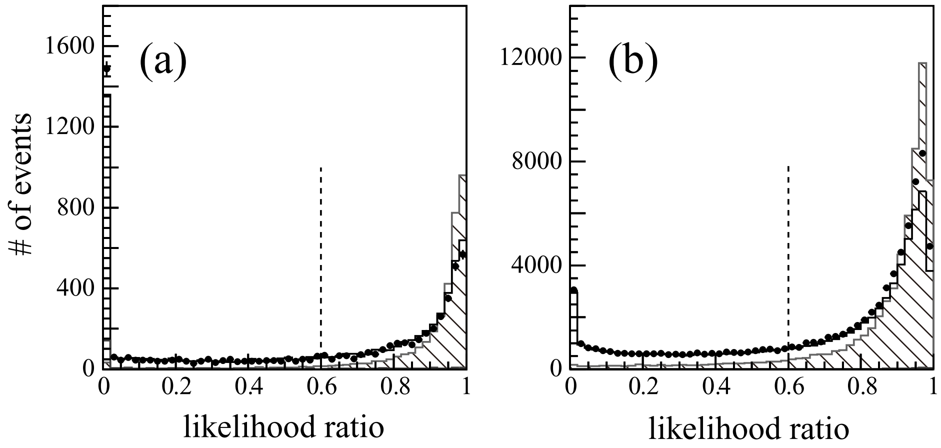

Fig. 2. Distribution of the likelihood ratio for (a) $K^-\pi^0\eta\nu_\tau$ and (b) $\pi^-\pi^0\eta\nu_\tau$. Dots are experimental data. The hatched and normal histograms indicate the signal and BG MC distributions, respectively. The dashed line shows the threshold of this selection.

3.2 $\tau^- \to K^-\pi^0\eta\nu_\tau$ *and* $\pi^-\pi^0\eta\nu_\tau$ *decays*

For these decays, an η is reconstructed through the $\gamma\gamma$ mode only, so that the signal event should contain one charged track and four γ's on the signal side.

All γ's, except for a possible extra γ, are required to be detected in the barrel region of the calorimeter, and two of them should form a combination consistent the π^0 mass. The total momentum on the signal side is required to satisfy $\sum p_{\rm sig}^{\rm CM} > 2.5$ GeV/c. A condition on the opening angle between the missing momentum in the CM and the thrust axis is imposed: $\cos\theta(\mathbf{p}_{\rm miss}^{\rm CM};\mathbf{n}_{\rm thrust}^{\rm sig}) < -0.6$, to remove BG's with large missing momentum on the signal side. Charged kaons and pions are selected by requiring large $\mathcal{P}_K$ and small $\mathcal{P}_e$ in the $K^-\pi^0\eta\nu_\tau$ mode, while small $\mathcal{P}_K$ and small $\mathcal{P}_e$ are selected in the $\pi^-\pi^0\eta\nu_\tau$ mode.

For further background rejection, we construct a likelihood using the following seven variables: $V_{\rm thrust}$, momenta of the η and π^0 in the CM ($p_\eta^{\rm CM}$, $p_{\pi^0}^{\rm CM}$), the missing-mass squared ($M_{\rm miss}^2$), the energy of the γ_η's in the CM ($E_{\gamma_\eta}^{\rm CM}$), $\sum p_{\rm sig}^{\rm CM}$, and $\cos\theta(p_{K/\pi}^{\rm CM};p_\eta^{\rm CM})$. The MC simulation is used to study the likelihood distributions of generic $\tau^+\tau^-$ and the small residual $q\bar{q}$ BG ($L_{\rm BG}$) as well as the signal ($L_{\rm sig}$). A likelihood ratio is defined as $R = L_{\rm sig}/(L_{\rm sig} + L_{\rm BG})$. The R distribution is shown in Figs. 2 (a) for $K^-\pi^0\eta\nu_\tau$ and (b) for $\pi^-\pi^0\eta\nu_\tau$ decay; with the requirement $R > 0.6$, about half of the background is removed, while 93% and 90% of the signal samples are retained, respectively.

The resulting $M_{\gamma\gamma}$ distributions are shown in Figs.3 (a) and (b) for the $K^-\pi^0\eta\nu_\tau$ and $\pi^-\pi^0\eta\nu_\tau$ modes, respectively. The η peaks are clearly visible. The detection efficiencies are $\epsilon = 0.35\%$ and 0.47% in the $\tau^- \to K^-\pi^0\eta\nu_\tau$ and $\pi^-\pi^0\eta\nu_\tau$

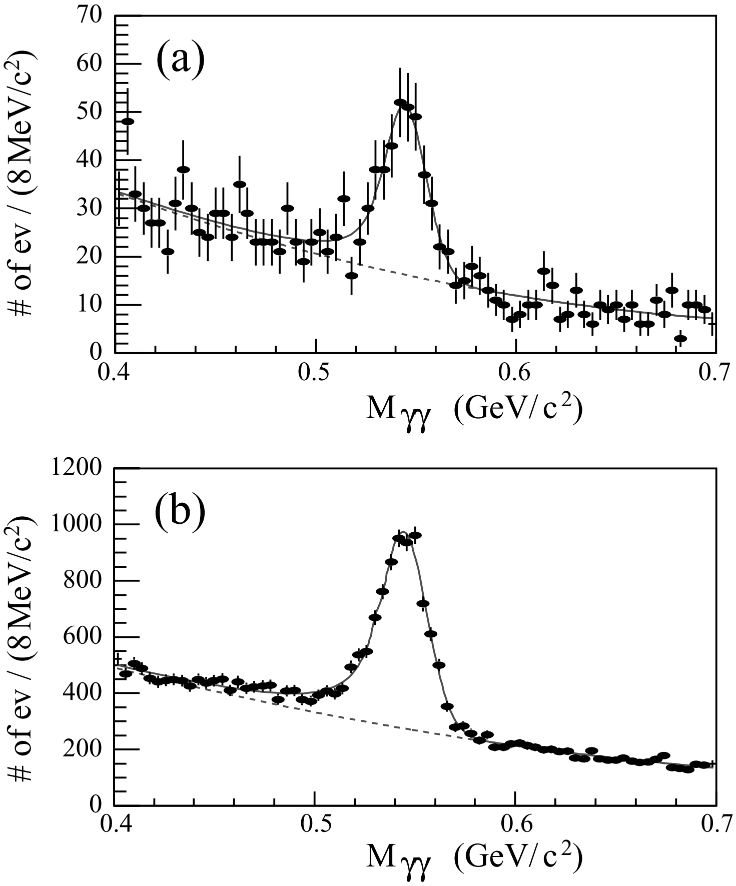

Fig. 3. $M_{\gamma\gamma}$ distributions for (a) $K^-\pi^0\eta\nu_\tau$ and (b) $\pi^-\pi^0\eta\nu_\tau$ candidates. Data are fit with a Crystal Ball function plus a second-order polynomial for the BG. The result of the best fit is indicated by the solid curve with the BG shown by the dashed curve.

decays, respectively.

3.3 $\pi^- K^0_S \eta\nu_\tau$ *decay*

On the signal side, three charged tracks and at least two γ's are required. To suppress two-photon BG, the tracks should not be identified as electrons. Without K/π ID the pion mass of $m_{\pi^\pm} = 0.13957$ GeV/c^2 is assigned to all three tracks on the signal side, two of the three tracks with opposite charges are the K^0_S daughters, the invariant mass ($M_{\pi^+\pi^-}$) of which is required to be within a K^0_S mass window (3σ), 0.4907 GeV/$c^2 < M_{\pi^+\pi^-} <$ 0.5047 GeV/c^2. To ensure that these tracks are K^0_S daughters, the distance from the interaction point to the K^0_S decay vertex on the plane perpendicular to the beam axis (r_{vertex}) is required to satisfy the condition: 0.5 cm $< r_{\text{vertex}} <$ 30 cm. To avoid multiple candidates, the mass of the other possible combination must not satisfy the K^0_S mass condition. Pairs of γ's with $E_\gamma > 0.3$ GeV are used to form η candidates. We require that the energy of an η candidate, E_η, must be greater than 1.2 GeV.

The resulting $M_{\gamma\gamma}$ distribution is shown in Fig.5 (a). The detection efficiency is $\epsilon = 0.32\%$, which includes the tag-side efficiency, $\mathcal{B}(\eta \to \gamma\gamma)$ and $\mathcal{B}(K_S^0 \to \pi^+\pi^-)$.

4 Branching Fractions

4.1 $K^-\eta\nu_\tau$, $K^-\pi^0\eta\nu_\tau$ *and* $\pi^-\pi^0\eta\nu_\tau$ *decays*

4.1.1 Signal candidates

The η meson yields are obtained from fits to the $\gamma\gamma$ invariant mass distributions shown in Figs.1 and 3. Fits are performed with a Crystal Ball (CB) function [18] plus a second-order polynomial function to represent the η contribution and combinatorial BG, respectively. All five parameters of the CB function, as well as three others for BG are treated as free parameters in the fit.

The results of the fit are shown by the solid curve in the corresponding figures. The best fits give η masses of $M_\eta = 0.5449 \pm 0.0006$, 0.5444 ± 0.0010 and 0.5443 ± 0.0004 GeV/c^2 for $K^-\eta\nu_\tau$, $K^-\pi^0\eta\nu_\tau$, and $\pi^-\pi^0\eta\nu_\tau$ decays, respectively, in the $\eta \to \gamma\gamma$ subsample, while $M_\eta = 0.5474 \pm 0.0007$ GeV/c^2 for $K^-\eta\nu_\tau$ in the $\eta \to \pi^+\pi^-\pi^0$ subsample. The corresponding mass resolutions are $\sigma_{M_\eta} = 0.0110 \pm 0.0006$, 0.0107 ± 0.0015, 0.0116 ± 0.0003, and 0.0075 ± 0.0004 GeV/c^2, respectively. These values of M_η and σ_{M_η} are in good agreement with those obtained from the MC simulation, although the obtained masses are shifted by 2 - 3 σ from the η mass in Ref. [17], which is due to the incomplete detector calibration. For instance, $M_\eta^{\rm MC} = 0.5442$, 0.5450, 0.5464, and 0.5473 GeV/c^2 for a generated mass of $m_\eta = 0.54745$ GeV/c^2.

The η yields obtained from the fits are $N_\eta = 1,387 \pm 43$, 270 ± 33, and $5,959 \pm 105$ events for the $K^-\eta\nu_\tau$, $K^-\pi^0\eta\nu_\tau$, and $\pi^-\pi^0\eta\nu_\tau$ modes, respectively, in the $\eta \to \gamma\gamma$ case, while $N_\eta = 241 \pm 21$ events for the $K^-\eta\nu_\tau$ decay in the $\eta \to \pi^+\pi^-\pi^0$ case. These yields include BG, attributed to other τ decays with η meson(s), such as the $\tau^- \to \pi^-\pi^0\pi^0\eta\nu_\tau$ and $\pi^-\pi^+\pi^-\eta\nu_\tau$; $q\bar{q}$ continuum with η meson(s); cross-feeds among the signal modes.

4.1.2 Background

The possible backgrounds in the $K^-\eta\nu_\tau$, $K^-\pi^0\eta\nu_\tau$ and $\pi^-\pi^0\eta\nu_\tau$ decay modes include (a) feed-across from signal modes and (b) other processes such as $\tau \to \pi^-\pi^0\pi^0\eta\nu_\tau$, $K^-\eta\eta\nu_\tau$, $\pi^-\eta\eta\nu_\tau$, $\pi^-\eta\nu_\tau$ and $q\bar{q}$. We first discuss the second source.

BG from generic $\tau^+\tau^-$ decays is evaluated using a MC simulation where the value of $\mathcal{B}(\tau^- \to \pi^-\pi^0\pi^0\eta\nu_\tau)$ is taken from Ref. [19]. This BG is negligible for $K^-\eta\nu_\tau$ and $K^-\pi^0\eta\nu_\tau$ decays, and is only 72 ± 20 events, which is smaller than the statistical uncertainty in the η yield for the $\pi^-\pi^0\eta\nu_\tau$ decay.

To examine the $\tau^- \to K^-\eta\eta\nu_\tau$ and $\pi^-\eta\eta\nu_\tau$ contaminations, we analyze data using selection criteria similar to those used for the $K^-\pi^0\eta\nu_\tau$ and $\pi^-\pi^0\eta\nu_\tau$ modes. An additional η, instead of a π^0, is reconstructed, and no selection on the likelihood ratio is implemented. Requiring one photon pair to be in the η mass region, $0.48\text{GeV}/c^2 < M_{\gamma\gamma}^{(1)} < 0.58\ \text{GeV}/c^2$, which includes the largest energy γ, the invariant mass distribution of the other η candidate, ($M_{\gamma\gamma}^{(2)}$), is shown in Figure 4. The evaluated η yields are $1.4^{+2.6}_{-1.9}$ and 4.4 ± 6.8 events in the $K^-\eta\eta\nu_\tau$ and $\pi^-\eta\eta\nu_\tau$ decays, respectively, with detection efficiencies of $\epsilon = 0.19\%$ and 0.22%, respectively. We then set the upper limits [20]

$$\mathcal{B}(\tau^- \to K^-\eta\eta\nu_\tau) < 3.0 \times 10^{-6} \tag{1}$$

and

$$\mathcal{B}(\tau^- \to \pi^-\eta\eta\nu_\tau) < 7.4 \times 10^{-6} \tag{2}$$

at the 90% confidence level (CL) including systematic uncertainties of 6.9% and 7.1%, respectively. Since the cross feed probability for these modes with extra η's is below 3%, their contamination is ignored.

The $\tau^- \to \pi^-\eta\nu_\tau$ decay proceeds via a second-class current so that its branching fraction is expected to be small, as low as 10^{-5} [3] or less. Since the efficiency for detecting $\pi^-\eta\nu_\tau$ as signal is of the order of 10^{-4}, the total contamination is then $\sim 10^{-9}$ or less so that this decay can be ignored.

BG from the $q\bar{q}$ continuum is examined using both MC and data in order to take into account the η production uncertainty of the $q\bar{q}$ MC. A $q\bar{q}$ enriched sample is produced with some variations of the signal selection criteria. We require $M_{\text{tag}} > m_\tau$, while the requirement $M_{\text{sig}} < m_\tau$ is not applied; the PID requirement on the tag side is reversed. Other criteria are not changed. A comparison between the resulting η yields of MC and the data resulted in the following MC scale factors: 2.3 ± 0.7 for $K^-\eta\nu_\tau$, 2.6 ± 0.5 for $K^-\pi^0\eta\nu_\tau$, and 2.9 ± 0.3 for $\pi^-\pi^0\eta\nu_\tau$. Therefore, we obtain rescaled $q\bar{q}$ contaminations of 39.7 ± 15.8 events in $K^-\eta\nu_\tau$, 212 ± 29 events in $\pi^-\pi^0\eta\nu_\tau$ and 27.0 ± 8.5 events

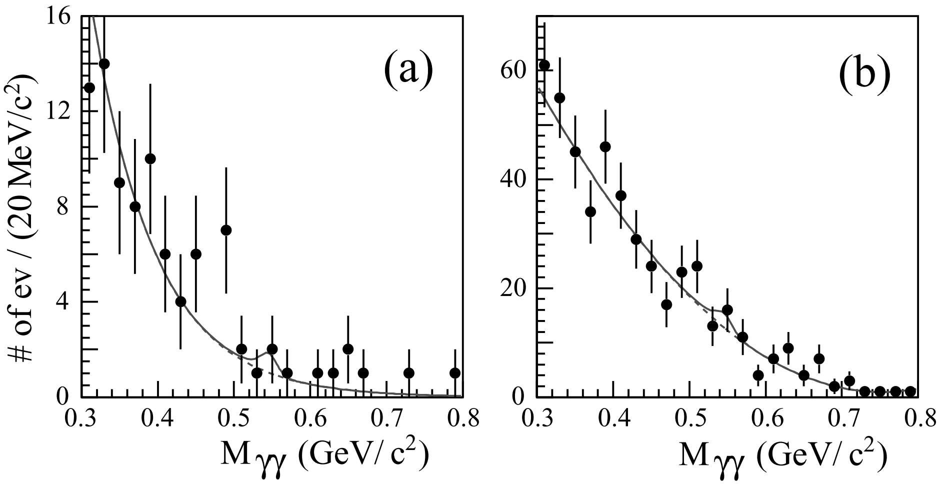

Fig. 4. Mass of the γ_η's combination, which does not include the largest energy γ_η, $M^{(2)}_{\gamma\gamma}$ for (a) the $\tau^- \to K^-\eta\eta\nu_\tau$ sample and (b) the $\tau^- \to \pi^-\eta\eta\nu_\tau$ sample. Data are fit with a Crystal Ball function plus a second-order polynomial for the BG. The result of the best fit is indicated by the solid curve with the BG shown by the dashed curve.

in the $K^-\pi^0\eta\nu_\tau$ decay. These BG's correspond to 2.8%, 10% and 3.6% of the raw signal yields, N_η, respectively.

The yields in the three candidate samples after the BG subtraction evaluated above, N_i, ($i = K^-\eta\nu$, $K^-\pi^0\eta\nu$, $\pi^-\pi^0\eta\nu$) are used to evaluate the corresponding branching fractions, $\mathcal{B}_i$. To take into account the cross-feeds between decay channels, we solve the following system of linear equations:

$$N_j = 2N_{\tau\tau}\sum_{i=1}^{3}\epsilon^i_j\mathcal{B}_i \qquad (j = 1, 2, 3), \tag{3}$$

where ϵ^i_j is the efficiency for detecting mode j as mode i, which is estimated by MC; $N_{\tau\tau}$ is the total number of τ-pairs produced. In the $\eta \to \pi^+\pi^-\pi^0$ case, $\mathcal{B}(\tau^- \to K^-\eta\nu_\tau)$ is calculated using the relation $N'_1 = 2N_{\tau\tau}\sum_{i=1}^{3}\epsilon'^i_1\mathcal{B}_i$ (the prime indicates quantities for this η mode) with $\mathcal{B}_2$ and $\mathcal{B}_3$ obtained in the $\eta \to \gamma\gamma$ case. The statistical uncertainty in N'_1 is $\sim 10\%$, while the cross-feed contamination is $\sim 4\%$, and is thus insignificant.

The resulting branching fractions are $\mathcal{B}(\tau^- \to K^-\eta\nu_\tau) = (1.57 \pm 0.05) \times 10^{-4}$, $\mathcal{B}(\tau^- \to K^-\pi^0\eta\nu_\tau) = (4.6 \pm 1.1) \times 10^{-5}$, and $\mathcal{B}(\tau^- \to \pi^-\pi^0\eta\nu_\tau) = (1.35 \pm 0.03) \times 10^{-3}$ in the $\eta \to \gamma\gamma$ case, and $\mathcal{B}(\tau^- \to K^-\eta\nu_\tau) = (1.60 \pm 0.15) \times 10^{-4}$ in the $\eta \to \pi^+\pi^-\pi^0$ case.

4.1.3 Systematic uncertainties

Systematic uncertainties are discussed below, and listed in Table 1.

Table 1
Summary of systematic uncertainties in each mode (%). The uncertainty in the number of $\tau^+\tau^-$ events comes from the uncertainties in our luminosity measurement by Bhabha events and the cross section of $e^+e^- \to \tau^+\tau^-$ [21].

Signal modes	$K^-\eta\nu$	$K^-\pi^0\eta\nu$	$\pi^-\pi^0\eta\nu$	$K^-\eta\nu$
Items	$\eta \to \gamma\gamma$			$\eta \to 3\pi$
BG subtraction				
$K^-\eta\nu_\tau$	–	0.6	1.8×10^{-3}	–
$K^-\pi^0\eta\nu_\tau$	0.3	–	4.2×10^{-2}	0.4
$\pi^-\pi^0\eta\nu_\tau$	7.5×10^{-2}	3.3	–	0.1
$\pi^-\pi^0\pi^0\eta\nu_\tau$	–	–	0.4	–
$q\bar{q}$	1.5	6.0	0.5	1.5
Detection efficiency				
K/π- /lepton-id	3.3/ 2.3	2.2/ 2.8	1.0/2.6	2.8/ 2.6
Tracking	1.3	1.3	1.3	3.3
$\pi^0/\eta \to \gamma\gamma$	–/ 2.0	2.0/ 2.0	2.0/ 2.0	2.0/ –
π^0 veto	2.8	2.8	2.8	–
Stat. error of signal MC	0.5	1.7	0.5	1.3
$\mathcal{B}(\eta \to \pi^+\pi^-\pi^0)$	–	–	–	1.6
Luminosity meas.	1.4			
$\sigma(e^+e^- \to \tau^+\tau^-)$	0.3			
Total	5.9	9.1	5.3	6.2

Subtraction of the BG discussed above provides the systematic uncertainties includes the statistical errors in the detection efficiencies for BG processes, as listed in the Table. Sizable uncertainties are found only in $K^-\pi^0\eta\nu$ decay from $\pi^-\pi^0\eta\nu_\tau$ and the $q\overline{q}$ continuum and amount to 3.3% and 6.0%, respectively.

The systematic uncertainties for PID, track finding, π^0 and η reconstruction, and the π^0-veto are also estimated. The modeling of the PID likelihood is tested by studying inclusive D^{*-} samples for K/π and two-photon $\gamma\gamma \to \ell^+\ell^-$ samples for leptons; the Uncertainty in the PID efficiency is 2-3%, 1% and $\sim$ 2.5% for $K^\pm$, $\pi^\pm$ and $(\mu/e)^\pm$, respectively. The uncertainty for finding a track is 1.0 % for hadrons and 0.3% for leptons. The uncertainty in $\pi^0/\eta \to \gamma\gamma$ reconstruction is 2.0%, obtained from a comparison of $\eta \to \gamma\gamma$ and $\eta \to \pi^0\pi^0\pi^0$ data samples. The π^0-veto inefficiency in $\pi^-\pi^0\eta\nu_\tau$ samples is evaluated by comparing its effect on the data and MC samples when the tag-side lepton-PID criterion is reversed from the ordinary selection.

The statistical errors on the MC simulation are 0.5%, 1.7% and 0.5% for $\tau^- \to K^-\eta\nu_\tau$, $K^-\pi^0\eta\nu_\tau$ and $\pi^-\pi^0\eta\nu_\tau$ in the $\eta \to \gamma\gamma$ case, respectively, and 1.3% for $\tau^- \to K^-\eta\nu_\tau$ in the $\eta \to \pi^+\pi^-\pi^0$ case. The branching fractions used in the MC are cited from Ref. [17], where $\mathcal{B}(\eta \to \pi^+\pi^-\pi^0)$ yields a sizable uncertainty of 1.6%, while others are negligible. The uncertainty of the $\sigma(e^+e^- \to \tau^+\tau^-)$ cross section and the integrated luminosity are 0.3% and 1.4%, respectively.

All contributions are summed up in quadrature to obtain the total uncertainties; they amount to 5.9%, 9.1% and 5.3% for $\mathcal{B}(\tau^- \to K^-\eta\nu_\tau)$, $\mathcal{B}(\tau^- \to K^-\pi^0\eta\nu_\tau)$ and $\mathcal{B}(\tau^- \to \pi^-\pi^0\eta\nu_\tau)$, respectively, in the $\eta \to \gamma\gamma$ case, and 6.2% for $\mathcal{B}(\tau^- \to K^-\eta\nu_\tau)$ in the $\eta \to \pi^+\pi^-\pi^0$ case.

Taking into account the systematic errors, we obtain the following branching fractions:

$$\begin{aligned}
&\mathcal{B}(\tau^- \to K^-\eta\nu_\tau) \\
&= (1.57 \pm 0.05 \pm 0.09) \times 10^{-4} \quad \text{for } \eta \to \gamma\gamma, && (4)\\
&= (1.60 \pm 0.15 \pm 0.10) \times 10^{-4} \quad \text{for } \eta \to \pi^+\pi^-\pi^0, && (5)\\
&\mathcal{B}(\tau^- \to K^-\pi^0\eta\nu_\tau) \\
&\qquad = (4.6\ \pm 1.1 \pm 0.4) \times 10^{-5}, && (6)\\
&\mathcal{B}(\tau^- \to \pi^-\pi^0\eta\nu_\tau) \\
&\qquad = (1.35 \pm 0.03 \pm 0.07) \times 10^{-3}. && (7)
\end{aligned}$$

For $K^-\eta\nu_\tau$, the two measurements are combined to obtain

$$\begin{aligned}
&\mathcal{B}(\tau^- \to K^-\eta\nu_\tau) \\
&\qquad = (1.58 \pm 0.05 \pm 0.09) \times 10^{-4}. && (8)
\end{aligned}$$

4.2 $\pi^-K^0_S\eta\nu_\tau$ decay

4.2.1 Signal candidates

For $\pi^-K^0_S\eta\nu_\tau$, the signal yield N_η is evaluated from a fit to the $M_{\gamma\gamma}$ mass distribution in the same way, as discussed in 4.1.1, but the parameters of the CB function are fixed to those determined by the signal MC simulation. The fit result is shown in Fig. 5 (a), yielding $N_\eta = 161 \pm 18$ events.

We examine $\tau^- \to K^-K^0_S\eta\nu_\tau$ and $\pi^-\pi^+\pi^-\eta\nu_\tau$ decays in order to determine their cross-feed contaminations, with selection criteria similar to those for $\pi^-K^0_S\eta\nu_\tau$. For $K^-K^0_S\eta\nu_\tau$, the charged track on the signal side is required to

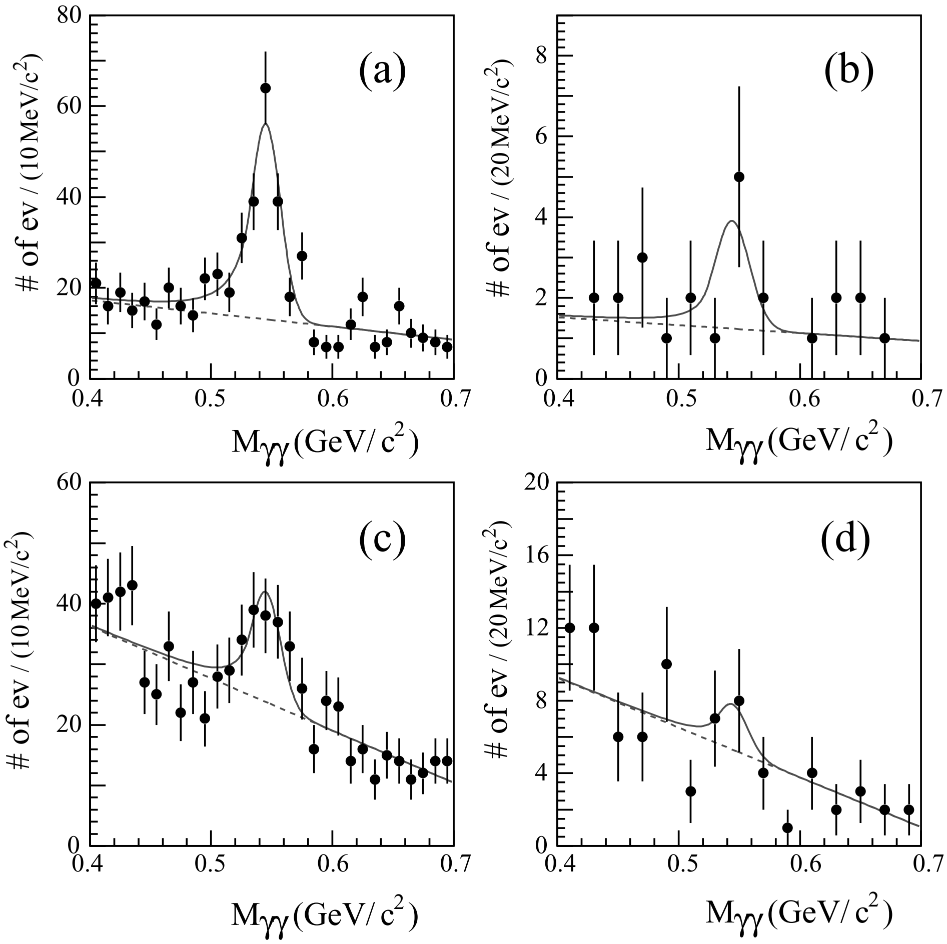

Fig. 5. $M_{\gamma\gamma}$ distributions for (a) $\pi^- K_S^0 \eta \nu_\tau$, (b) $K^- K_S^0 \eta \nu_\tau$, (c) $\pi^-\pi^+\pi^-\eta\nu_\tau$ without a K_S^0, and (d) $\pi^-\pi^0 K_S^0 \eta \nu_\tau$ samples. Data are fit with a Crystal Ball function plus a second-order polynomial for the BG. The result of the best fit is indicated by the solid curve with the BG shown by the dashed curve.

be a kaon; $N_\eta = 5.6 \pm 3.6$ events is obtained from the fit (see Fig.5 (b)). For $\tau^- \to \pi^-\pi^+\pi^-\eta\nu_\tau$, its $M_{\gamma\gamma}$ mass distribution, as shown in Fig. 5 (c), is formed from a sample in which the $\pi^+\pi^-$ invariant mass lies outside the K_S^0 mass range while the other requirements for K_S^0 daughters are the same; the fit gives $N_\eta = 67.9 \pm 17.0$ events.

4.2.2 Background

The possible background to the signal comes from $\pi^-\pi^0 K_S^0 \eta \nu_\tau$ and the $q\overline{q}$ continuum. The former sample is selected, requiring an additional π^0 on the signal side. No clear η peak is found in the $M_{\gamma\gamma}$ distribution, as can be seen in Fig. 5 (d): $N_\eta = 4.7^{+6.0}_{-5.1}$ events is obtained with a detection efficiency of $\epsilon = 0.08\%$. We therefore set an upper limit on the branching fraction $\mathcal{B}(\tau^- \to \pi^- K_S^0 \pi^0 \eta \nu_\tau) < 2.5 \times 10^{-5}$ at the 90% CL. The BG from this mode in the

$\pi^- K_S^0 \eta\nu_\tau$ sample is calculated to be $1.6^{+2.0}_{-1.7}$ events.

The contamination of $q\bar{q}$ in $\pi^- K_S^0 \eta\nu_\tau$ decay is 21.1 ± 7.5 events, following from MC simulation with a scale factor estimated from the $q\bar{q}$ enriched sample.

After subtracting the two above BG's from the yield N_η for $\pi^- K_S^0 \eta\nu_\tau$ decay, we solve the simultaneous equations of Eq.(3) in order to take into account the cross-feeds among the three modes. Now, the (super)subscripts $i, j = 1, 2, 3$ for the equations correspond to $1 = \pi^- K_S^0 \eta\nu_\tau$, $2 = K^- K_S^0 \eta\nu_\tau$, $3 = \pi^-\pi^+\pi^-\eta\nu_\tau$. The last category includes other peaking BG from generic τ decays, which are estimated using samples in the K_S^0 sidebands. The detection efficiencies are, for instance, $\epsilon_1^1 = 0.32\%$ and $\epsilon_2^2 = 0.23\%$. The resulting branching fractions are $\mathcal{B}(\tau^- \to \pi^- K_S^0 \eta\nu_\tau) = (4.38 \pm 0.75) \times 10^{-5}$ and $\mathcal{B}(\tau^- \to K^- K_S^0 \eta\nu_\tau) = (1.9 \pm 2.0) \times 10^{-6}$, respectively.

4.2.3 Systematic uncertainties

Systematic errors for $\mathcal{B}(\tau^- \to \pi^- K_S^0 \eta\nu_\tau)$ include the following sources. Uncertainty in the signal CB function used to fit the $M_{\gamma\gamma}$ spectrum is examined by varying M_η and σ_{M_η} within their errors: the fitted yield N_η varies by 0.7%. The dominant BG comes from the $q\bar{q}$ continuum: its uncertainty is evaluated to be 6.2%, while that of the others is negligible. The uncertainties in the luminosity evaluation and $\sigma(e^+e^- \to \tau^+\tau^-)$ are 0.3% and 1.4%, respectively. The value of $\mathcal{B}(K_S^0 \to \pi^+\pi^-)$ used in MC has a 0.4% error [17]. The uncertainty in the CB function yields a 0.5% contribution. The total systematic uncertainty is consequently calculated to be 7.9%, by adding all of the above errors in quadrature.

As a result, we obtain the following branching fractions:

$$\begin{aligned} &\mathcal{B}(\tau^- \to \pi^- K_S^0 \eta\nu_\tau) \\ &\qquad = (4.4 \pm 0.7 \pm 0.3) \times 10^{-5}, \end{aligned} \tag{9}$$

and

$$\mathcal{B}(\tau^- \to K^- K_S^0 \eta\nu_\tau) < 4.5 \times 10^{-6}, \tag{10}$$

at the 90% CL.

4.3 $\tau^- \to K^{*-}\eta\nu_\tau$ decay

The $(K\pi)^-$ invariant mass spectra in both $\tau^- \to K^-\pi^0\eta\nu_\tau$ and $\tau^- \to \pi^- K_S^0 \eta\nu_\tau$ decays are analyzed to determine the $K^*(892)^-$ content in the final state.

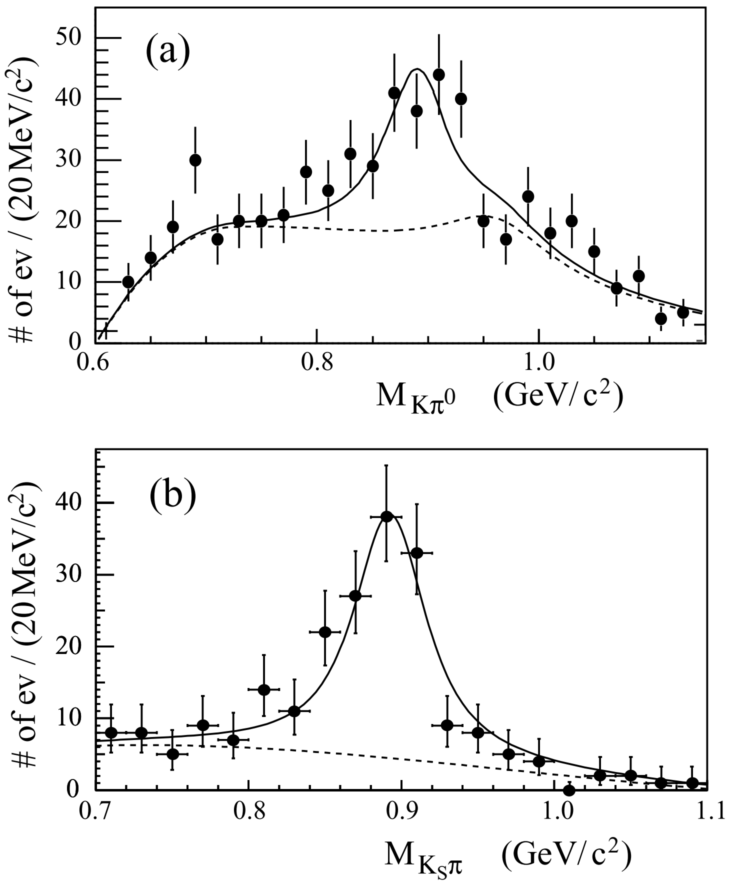

Fig. 6. (a) $K^-\pi^0$ invariant mass distribution for $K^-\pi^0\eta\nu_\tau$ events and (b) the $\pi^-K_S^0$ invariant mass distribution for $\pi^-K_S^0\eta\nu_\tau$ events. Data are fitted with a convoluted Breit-Wigner function, and the best fit is indicated by the solid curve, while the BG component is shown by the dashed curve. The fits give $N_{K^{*-}\eta\nu_\tau} = 122 \pm 17$ events (a) and $N_{K^{*-}\eta\nu_\tau} = 123 \pm 14$ (b), respectively.

4.3.1 $\tau^- \to K^-\pi^0\eta\nu_\tau$ *samples*

To select $\tau^- \to K^-\pi^0\eta\nu_\tau$, the η signal is identified with the criterion $0.50\ \mathrm{GeV}/c^2 < M_{\gamma\gamma} < 0.58\ \mathrm{GeV}/c^2$, and then the $K^-\pi^0$ invariant mass $M_{K^-\pi^0}$ distribution is analyzed (see Fig. 6 (a)). The contribution of the combinatorial BG under the η peak is evaluated from the sidebands with $0.43\ \mathrm{GeV}/c^2 < M_{\gamma\gamma} < 0.48\ \mathrm{GeV}/c^2$ and $0.60\ \mathrm{GeV}/c^2 < M_{\gamma\gamma} < 0.65\ \mathrm{GeV}/c^2$. The dashed curve in Fig. 6 (a) indicates the BG component estimated from the above samples and from MC that includes a τ decay with an η. A MC study indicates that the enhancement in the higher $M_{K^-\pi^0}$ mass region mostly arises from $\pi^-\pi^0\eta\nu_\tau$ events through misidentification of $\pi^- \to K^-$, while the dominant BG, mostly populating the lower mass region, is composed of contributions from generic τ decays. A clear $K^*(892)^-$ signal over BG can be seen in the spectrum shown in Fig. 6 (a).

The observed $M_{K^-\pi^0}$ spectrum is fitted with a K^* Breit-Wigner (BW) function plus a BG component, where the former is convoluted with a response function with a mass resolution of $\sigma_{M_{K^-\pi^0}} = 13.5$ MeV/c^2. The latter is fixed so as to reproduce the $M_{K^-\pi^0}$ spectrum of the sidebands. The mass and width of the BW function are fixed to those of the $K^*(892)^-$ [17] in the fit. The best-fit result is indicated by the solid curve in the figure, and gives $N_{K^{*-}\eta\nu_\tau} = 122 \pm 17$ events with a $\chi^2/\text{d.o.f} = 27.4/27$.

We examine the non-resonant $K^-\pi^0$ contamination by adding an additional term in the fit, assuming a phase-space distribution with a $V - A$ weak interaction for a hadronic final system. The fit gives $N_{K^{*-}\eta\nu_\tau} = 104 \pm 20$ events and $N_{\text{non}-\text{K}^{*-}} = 42 \pm 25$ events with a $\chi^2/\text{d.o.f} = 24.5/26$. Since no significant difference between the two fits is found within the errors, we here simply take the intermediate state to be purely $K^{*-}\eta\nu_\tau$ and the difference is taken into account as the systematic uncertainty for the fitting function. Even allowing for interference between the K^{*-} and non-resonant $K^-\pi^0$, the difference is found to be negligible.

No significant $K^*(892)^-$ BG contribution is found in generic τ decays, while 6.5 ± 2.3 events are estimated from the $q\bar{q}$ MC.

The detection efficiency is evaluated from MC as $\epsilon = 0.12\%$, including the branching fractions for $K^*(892)^- \to K^-\pi^0$ and $\eta \to \gamma\gamma$ decays.

The systematic uncertainties in the evaluation of $\mathcal{B}(K^*(892)^-\eta\nu_\tau)$ are summarized in Table 2. The dominant error arises from the uncertainty in the fitting function discussed above. It amounts to 15%. Other sources of systematic uncertainties are the same as those for $K^-\pi^0\eta\nu_\tau$ decay. The total systematic uncertainty is 16.2%.

Thus we obtain the branching fraction

$$\begin{aligned}\mathcal{B}(\tau^- \to K^*(892)^-\eta\nu_\tau)_{K^{*-}\to K^-\pi^0} \\ = (1.13 \pm 0.17 \pm 0.18) \times 10^{-4}.\end{aligned} \tag{11}$$

For the non-resonant $K^-\pi^0\eta\nu_\tau$ decay, we set an upper limit on its branching fraction

$$\mathcal{B}(\tau^- \to K^-\pi^0\eta\nu_\tau)_{\text{non-resonant}} < 3.5 \times 10^{-5} \tag{12}$$

at the 90% CL, assuming a pure phase-space distribution for the final hadronic system.

4.3.2 $\tau^- \to K_S^0\pi^-\eta\nu_\tau$ samples

The $M_{K_S^0\pi^-}$ distribution is shown in Fig. 6(b) and is similar to the $M_{K^-\pi^0}$ case. A clear $K^*(892)^-$ signal can be seen over a small continuum BG.

Table 2
Summary of the systematic uncertainties in $K^{*-}\eta\nu_\tau$ analysis (%).

$K^*(892)^-$ decay mode	$K^-\pi^0$	$K^0_S\pi^-$
BG subtraction		
$q\bar{q}$	2.0	–
Detection efficiency		
K/π- /lepton-id	2.2/ 2.5	–/ 2.4
Tracking	1.3	3.3
$\pi^0/\eta \to \gamma\gamma$	2.0/ 2.0	–/ 2.0
π^0-veto	2.8	–
Stat. error of signal MC	1.7	0.7
$\mathcal{B}(K^0_S \to \pi^+\pi^-)$	–	0.1
Mass spectrum	0.5	0.5
Luminosity meas.	1.4	
$\sigma(e^+e^- \to \tau^+\tau^-)$	0.3	
Fitting function	15.0	4.1
Total	16.2	6.4

Assuming no non-resonant $K^0_S\pi^-$ contribution, the distribution is fitted with a convoluted BW function plus a BG, composed of a third-order polynomial, applying the same method used for the $K^-\pi^0\eta\nu_\tau$ sample. The yield of $K^*(892)^-$ is 123 ± 14 events. The K^{*-} BG is estimated to be 14.5 ± 5.0 events from the $q\bar{q}$ continuum, and is subtracted from the above yield.

We examine a possible non-resonant $K^0_S\pi^-$ contribution, whose mass spectrum is calculated by MC, assuming a pure hadronic phase-space distribution with a $V - A$ weak interaction. Including the non-resonant component, the best fit gives $N_{K^{*-}} = 121 \pm 16$ events and $N_{\mathrm{non-resonant}} = 3 \pm 15$ events. Therefore, we give results assuming no non-resonant background.

The detection efficiency is evaluated by MC as $\epsilon = 0.10\%$, which includes the relevant branching fractions: $\mathcal{B}(K^*(892)^- \to \pi^- K^0_S)$, $\mathcal{B}(K^0_S \to \pi^+\pi^-)$, and $\mathcal{B}(\eta \to \gamma\gamma)$.

The systematic uncertainties are summarized in Table 2. Their magnitudes are similar to those in the $K^-\pi^0\eta\nu_\tau$ case, except for the non-resonant contribution. The total systematic uncertainty is 6.4%. Consequently, the branching fraction

Table 3
Comparison with previous results.

	Branching fraction $\mathcal{B}$ ($\times 10^{-4}$)		
Mode	This work	Previous exp.	Reference
$\tau^- \to K^- \eta \nu_\tau$	$1.58 \pm 0.05 \pm 0.09$	$2.6 \pm 0.5 \pm 0.5$	CLEO [7]
		$2.9 \pm 1.3 \pm 0.7$	ALEPH [9]
$\tau^- \to \pi^- \pi^0 \eta \nu_\tau$	$13.5 \pm 0.3 \pm 0.7$	$17 \pm 2 \pm 2$	CLEO [6]
		$18 \pm 4 \pm 2$	ALEPH [9]
$\tau^- \to K^- \pi^0 \eta \nu_\tau$	$0.46 \pm 0.11 \pm 0.04$	$1.77 \pm 0.56 \pm 0.71$	CLEO [8]
$\tau^- \to \pi^- K_S^0 \eta \nu_\tau$	$0.44 \pm 0.07 \pm 0.02$	$1.10 \pm 0.35 \pm 0.11$	CLEO [8]
$\tau^- \to K^{*-} \eta \nu_\tau$	$1.34 \pm 0.12 \pm 0.09$	$2.90 \pm 0.80 \pm 0.42$	CLEO [8]

is

$$\begin{aligned}&\mathcal{B}(\tau^- \to K^*(892)^- \eta \nu_\tau)_{K^{*-} \to \pi^- K_S^0} \\ &\qquad = (1.46 \pm 0.16 \pm 0.09) \times 10^{-4}. \end{aligned} \tag{13}$$

Two measurements using $K^*(892)^- \to K^- \pi^0$ and $K_S^0 \pi^-$ decays are in agreement, in accordance with isospin symmetry. Therefore we combine the two results and obtain

$$\begin{aligned}&\mathcal{B}(\tau^- \to K^*(892)^- \eta \nu_\tau) \\ &\qquad = (1.34 \pm 0.12 \pm 0.09) \times 10^{-4}. \end{aligned} \tag{14}$$

5 Result

Using a high statistics 450 million τ-pair data sample from Belle, we have obtained the following branching fractions for five different decay modes:

$$\begin{aligned}
\mathcal{B}(\tau^- \to K^- \eta \nu_\tau) &= (1.58 \pm 0.05 \pm 0.09) \times 10^{-4}, \\
\mathcal{B}(\tau^- \to \pi^- \pi^0 \eta \nu_\tau) &= (1.35 \pm 0.03 \pm 0.07) \times 10^{-3}, \\
\mathcal{B}(\tau^- \to K^- \pi^0 \eta \nu_\tau) &= (4.6 \pm 1.1 \pm 0.4) \times 10^{-5}, \\
\mathcal{B}(\tau^- \to \pi^- K_S^0 \eta \nu_\tau) &= (4.4 \pm 0.7 \pm 0.3) \times 10^{-5}, \\
\mathcal{B}(\tau^- \to K^*(892)^- \eta \nu_\tau) &= (1.34 \pm 0.12 \pm 0.09) \times 10^{-4},
\end{aligned}$$

where the first and second errors are statistical and systematic, respectively. We also set the upper limits on the following decay modes at the 90% CL:

$$\mathcal{B}(\tau^- \to K^- K_S^0 \eta \nu_\tau) < 4.5 \times 10^{-6},$$

$$\mathcal{B}(\tau^- \to \pi^- K_S^0 \pi^0 \eta \nu_\tau) < 2.5 \times 10^{-5},$$
$$\mathcal{B}(\tau^- \to K^- \eta\eta \nu_\tau) < 3.0 \times 10^{-6},$$
$$\mathcal{B}(\tau^- \to \pi^- \eta\eta \nu_\tau) < 7.4 \times 10^{-6},$$
$$\mathcal{B}(\tau^- \to K^- \pi^0 \eta \nu_\tau)_{\mathrm{non-resonant}} < 3.5 \times 10^{-5}.$$

In Table 3, our results are compared to those previously obtained by the CLEO [6,7,8] and ALEPH [9] collaborations. It is clearly seen that the precision of the measured values has been considerably improved.

It is also noteworthy that the central values of our branching fractions are in all modes lower than those of the other experiments [6,7,8,9]. This fact can be mostly attributed to the underestimation of the BG contamination in previous low statistics measurements. For instance, the $q\bar{q}$ BG estimation in the previous analyses relied on the MC. However, this analysis evaluates the BG rate using a $q\bar{q}$ enriched data sample. Furthermore, Ref. [7] ignored the $K^-\pi^0\eta\nu_\tau$ BG contribution, since they estimated it as $\sim 0.1\%$ BG, based on a theoretical calculation that predicted its branching fraction to be 8.8×10^{-6} [3]. However, its rate is about 1% of the signal in our measurement, and its branching fraction is about five times as large. Our high statistics allows us to reliably and precisely scrutinize various BG contributions, while the previous measurements, which had low statistics, did not have sufficient sensitivity to notice, or correctly judge, the BG contamination.

Our results are compared with different theoretical calculations in Table 4. The branching fraction for $\tau^- \to \pi^-\pi^0\eta\nu_\tau$ decay can be predicted by the isospin symmetry (CVC) using the experimental results on $e^+e^- \to \pi^+\pi^-\eta$ [5,22]. Our branching fraction agrees with the predictions, $\mathcal{B}(\tau^- \to \pi^-\pi^0\eta\nu_\tau) = (1.3 \pm 0.2) \times 10^{-3}$ [5] and 1.5×10^{-3} [22].

Pich [3], Braaten [23], Li [4] and Aubrecht [24] calculated the branching fractions of various τ decays involving η meson(s), based on chiral perturbation theory, as listed in Table 4. Their results are in fair agreement with our measurements, particularly taking into account possible uncertainties in theoretical predictions. Further detailed studies of the physical dynamics in τ decays with η mesons are required.

It should be mentioned that the TAUOLA MC program [14] qualitatively reproduces our hadronic mass distributions in $\tau^- \to \pi^-\pi^0\eta\nu$, $\tau^- \to K^-\eta\nu$ and $\tau^- \to K^*(892)^-\eta\nu$ decays, as shown in Fig. 7. Further analysis of the spectra including various phenomenological models is in progress.

Acknowledgments

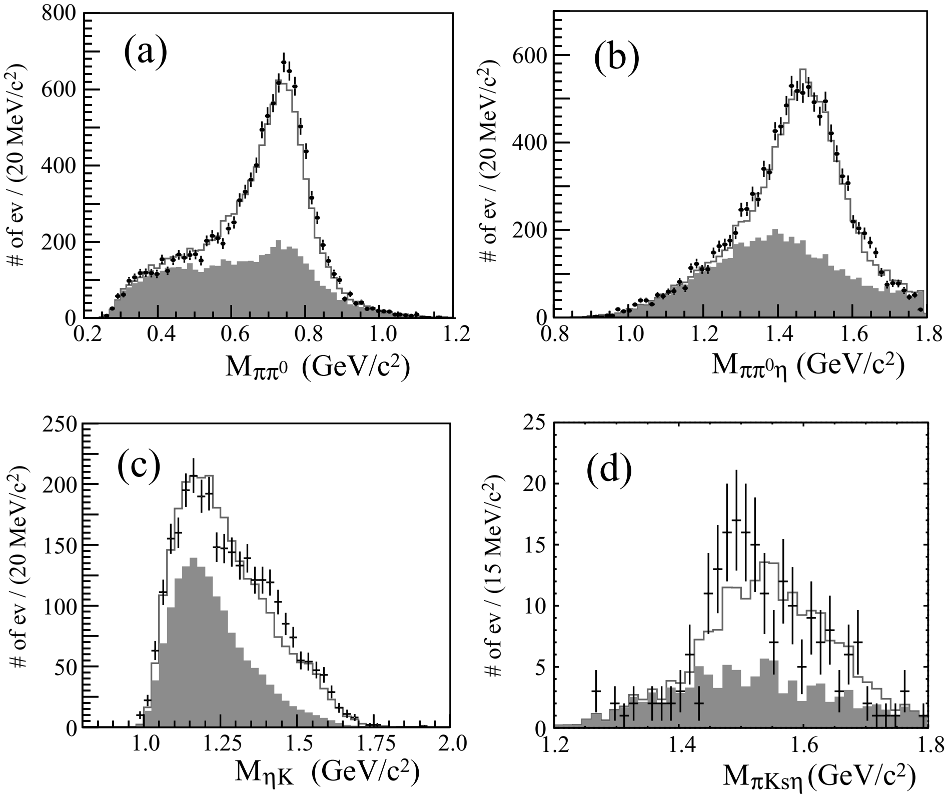

Fig. 7. Invariant mass distributions of (a) $\pi^-\pi^0$ and (b) $\pi^-\pi^0\eta$ for $\tau^- \to \pi^-\pi^0\eta\nu_\tau$ decay, (c) $K^-\eta$ for $\tau^- \to K^-\eta\nu_\tau$ and (d) $\pi^- K^0_S\eta$ for $\tau^- \to K^{*-}\eta\nu_\tau$, $K^{*-} \to K^0_S\pi^-$. The points with error bars are the data. The normal and filled histograms indicate the signal and $\tau\tau$ BG MC distributions, respectively. The $q\overline{q}$ BG is strongly suppressed and negligible in our sample.

We thank the KEKB group for the excellent operation of the accelerator, the KEK cryogenics group for the efficient operation of the solenoid, and the KEK computer group and the National Institute of Informatics for valuable computing and SINET3 network support as well as Tau lepton physics research center of Nagoya University. We acknowledge support from the Ministry of Education, Culture, Sports, Science, and Technology of Japan and the Japan Society for the Promotion of Science; the Australian Research Council and the Australian Department of Education, Science and Training; the National Natural Science Foundation of China under contract No. 10575109 and 10775142; the Department of Science and Technology of India; the BK21 program of the Ministry of Education of Korea, the CHEP src program and Basic Research program (grant No. R01-2008-000-10477-0) of the Korea Science and Engineering Foundation; the Polish State Committee for Scientific Research; the Ministry of Education and Science of the Russian Federation and the Russian Federal Agency for Atomic Energy; the Slovenian Research Agency; the Swiss National Science Foundation; the National Science Council and the Ministry of Education of Taiwan; and the U.S. Department of Energy. This work is supported by a Grant-in-Aid for Science Research on Priority Area (New Development of Flavor Physics) from the Ministry of Education, Culture, Sports, Science and Technology of Japan and Creative Scientific Research (Evolution of Tau-lepton Physics) from the Japan Society for the Promotion of Science.

References

[1] J. Wess and B. Zumino, Phys. Lett. B **37** (1971) 95.

[2] E. Witten, Nucl. Phys. B **223** (1983) 422.

[3] A. Pich, Phys. Lett. B **196** (1987) 561.

[4] B. A. Li, Phys. Rev. D **55** (1997) 1436.

[5] S. Eidelman and V. Ivanchenko, Phys. Lett. B **257** (1991) 437.

[6] CLEO Collaboration, M. Artuso et al., Phys. Rev. Lett. **69** (1992) 3278.

[7] CLEO Collaboration, J. Bartelt et al., Phys. Rev. Lett. **76** (1996) 4119.

[8] CLEO Collaboration, M. Bishai et al., Phys. Rev. Lett. **82** (1999) 281.

[9] ALEPH Collaboration, D. Buskulic et al., Z. Phys. C **74** (1997) 263.

[10] S. Kurokawa and E. Kikutani, Nucl. Instr. and Meth. A **499** (2003) 1, and other papers included in this volume.

[11] Belle Collaboration, A. Abashian et al., Nucl. Instr. and Meth. A **479** (2002) 117.

[12] Z. Natkaniec *et al.* (Belle SVD2 Group), Nucl. Instr. and Meth. A **560** (2006) 1.

[13] K. Hanagaki et al., Nucl. Instr. and Meth. A **485** (2002) 490;
A. Abashian et al., Nucl. Instr. and Meth. A **491** (2002) 69;
E. Nakano et al., Nucl. Instr. and Meth. A **494** (2002) 402.

[14] S. Jadach, B. F. L. Ward, Z. Wąs, Comp. Phys. Commun. **130** (2000) 260.

[15] D. J. Lange, Nucl. Instr. Meth. Phys. Res. Sect. A **462** (2001) 152.

[16] CERN Program Library Long Writeup No. W5013 1993.

[17] C. Amsler et al. (Particle Data Group), Phys. Lett. B **667** (2008) 1.

[18] J. E. Gaiser, Ph.D. thesis, SLAC-R-255 (1982).

[19] CLEO Collaboration, A. Anastassov et al., Phys. Rev. Lett. **86** (2001) 4467.

[20] The upper limit is estimated by following the method described in Ref. [17] section 32.3.2.4.

[21] S. Banerjee et al., Phys. Rev. D **77** (2008) 054012.

[22] F. J. Gilman, Phys. Rev. D **35** (1987) 3541.

[23] E. Braaten, R. J. Oakes and S. M. Tse, Phys. Rev. D **36** (1987) 2188.

[24] G. J. Aubrecht, N. Chahrouri and K. Slanec, Phys. Rev. D **24** (1981) 1318.

Table 4
Comparison with theoretical calculations

	Branching fractions					
Mode	This work	Pich [3]	Gilman [22]	Braaten [23]	Li [4]	Aubrecht [24]
$\tau^- \to K^- \eta \nu_\tau$	$(1.58 \pm 0.05 \pm 0.09) \times 10^{-4}$	1.2×10^{-4}			2.2×10^{-4}	1.6×10^{-4}
$\tau^- \to \pi^- \pi^0 \eta \nu_\tau$	$(1.35 \pm 0.03 \pm 0.07) \times 10^{-3}$	3×10^{-3}	1.5×10^{-3}	1.4×10^{-3}	1.9×10^{-3}	
$\tau^- \to K^- \pi^0 \eta \nu_\tau$	$(4.6 \pm 1.1 \pm 0.4) \times 10^{-5}$	8.8×10^{-6}				7.6×10^{-6}
$\tau^- \to \pi^- K_S^0 \eta \nu_\tau$	$(4.4 \pm 0.7 \pm 0.3) \times 10^{-5}$	1.1×10^{-5}				1.0×10^{-5}
$\tau^- \to K^{*-} \eta \nu_\tau$	$(1.34 \pm 0.12 \pm 0.09) \times 10^{-4}$				1.0×10^{-4}	
$\tau^- \to K^- K_S^0 \eta \nu_\tau$	$< 4.5 \times 10^{-6}$	1.6×10^{-7}				1.4×10^{-7}
$\tau^- \to \pi^- K_S^0 \pi^0 \eta \nu_\tau$	$< 2.5 \times 10^{-5}$					
$\tau^- \to K^- \eta \eta \nu_\tau$	$< 3.0 \times 10^{-6}$	1.6×10^{-9}				6.9×10^{-9}
$\tau^- \to \pi^- \eta \eta \nu_\tau$	$< 7.4 \times 10^{-6}$	1.1×10^{-9}				